Microsyst Technol (2012) 18:917–924
DOI 10.1007/s00542-011-1411-y

TECHNICAL PAPER

Selective modal excitation in coupled piezoelectric microcantilevers

M. Gil · T. Manzaneque · J. Hernando-García · A. Ababneh · H. Seidel · J. L. Sánchez-Rojas

Received: 28 July 2011 / Accepted: 20 December 2011 / Published online: 7 January 2012

Abstract We study in detail the first vibration modes of a piezoelectric resonator based on two coupled micro-cantilevers, also known as tuning-forks. A multiple electrode geometry lying on a layer of piezoelectric AlN allows the selective excitation of different modes, including in-plane modes. A complete optical characterization of the devices in the z- and also the x-direction has been performed employing a Doppler vibrometer. The measurements confirm the excitation and inhibition of different modes depending on the actuation signals distribution on the electrodes. The influence of the dimensions of the resonator on the coupling between the microcantilevers has also been studied. Quality factors above 4,300 have been measured for the first anti-phase in-plane mode.

1 Introduction

Micro-electro-mechanical systems (MEMS) resonators have aroused a great interest in recent years, especially those employed for sensing applications. The quality factor (Q-factor) of the resonators in one of their most important characteristics; high values of the Q-factor ensure good frequency stability and, thus, sensing resolution. Moreover, many biochemical sensing applications entail liquid media involving high viscous losses, requiring again high values of the Q-factor. In-plane modes have shown a better performance in viscous media, given that the damping for those modes is lower than for out-of-plane modes (Dufour et al. 2007). In this work we study in-plane and out-of-plane modes of coupled microcantilevers, including phase and anti-phase modes (Karrai and Grober 2005), as well as the best excitation configuration for each of the modes of interest. Oscillator circuits regularly include this kind of structures at the millimetric scale (Momosaki 1997). We study the performance of similar devices in micro scale for MEMS applications.

M. Gil (✉) · T. Manzaneque · J. Hernando-García · J. L. Sánchez-Rojas
Dpto. de Ingeniería Eléctrica, Electrónica, Automática y Comunicaciones, ETSI Industriales, Campus Universitario, 13071 Ciudad Real, Spain
e-mail: marta.gil@uclm.es

A. Ababneh
Electronic Engineering Department, Hijjawi Faculty for Engineering Technology, Yarmouk University, Irbid, Jordan

H. Seidel
Micromechanics, Microfluidics and Microactuators, Faculty of Natural Sciences and Technology II, Saarland University, 66123 Saarbrücken, Germany

2 Micro-resonator

The resonator we present here has been specifically designed to selectively stimulate or inhibit certain vibration modes. It consists of two coupled microcantilevers with the same dimensions forming a tuning-fork (see Fig. 1). The length and width of each of the arms are $L = 400$ μm and $w = 100$ μm, respectively. The rectangular coupling area (with dimensions s and d) acts as a junction with the holding frame (anchor). A thin layer of piezoelectric aluminum nitride (AlN) was deposited on the silicon substrate. Thus, the tuning fork resonances can be electrically actuated and sensed. For this purpose, a patterned aluminum electrode suitable for differential actuation has been fabricated. This split electrode has been designed to control the actuation of the first order in-plane modes, following a previously published optimization protocol (Sánchez-Rojas

et al. 2010). It consists of four individual electrodes distributed along the two arms of the resonator. Two parallel electrodes lie longitudinally on each of the arms and they can be excited independently with respect to the conducting silicon substrate which acts as one common reference bottom electrode. By this means, diverse actuation configurations can be applied, allowing the excitation of different vibration modes.

We have designed, fabricated and characterized several tuning forks with different geometries. The dimensions *s* and *d* of the anchor area have been varied in order to study its effect on the resonance frequency and the quality factor. In total, we considered five samples with different dimensions, which are shown in Table 1.

3 Mode selection

The main purpose of this design is the displacement optimization of the in-plane modes of the resonator, although in this work we mainly study the first six modes of the resonator, which include in-plane (IP) and out-of-plane (OP), as well as phase (P) and anti-phase (AP) modes (see Fig. 2). Numbers indicate the order of the mode.

For each mode there is an optimal signal distribution on the electrodes, expected according to the symmetry of the modal shape (see Fig. 2), which maximizes the respective displacement in z and x directions. This is indicated under the mode names in Tables 2 and 3.

To excite each of the four parts of the electrode we use two signals shifted 180°. For simplicity, we will refer to them as (+) and (−). The optimal signal configuration can be deduced from the stress distribution on the device (considering the plane stress components σ_{xx} and σ_{yy}), which involves the compression and expansion of each of the arms of the resonator for each mode. As previously

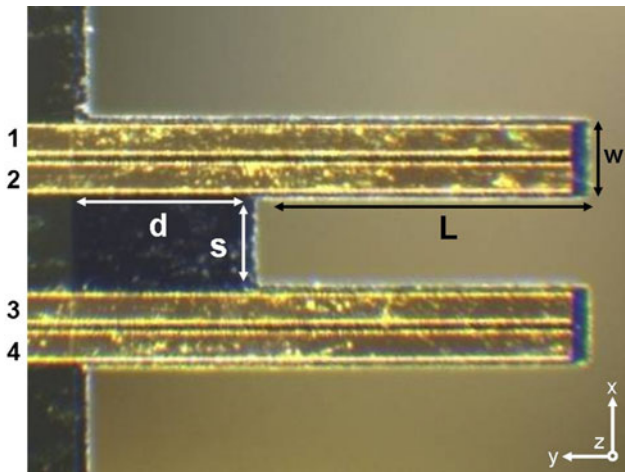

Fig. 1 Photograph of the device. The main dimensions (*L*, *d*, *s* and *w*) are indicated. *1*, *2*, *3* and *4* represent the four electrodes along the prongs of the fork

Table 1 Nominal dimensions of the studied resonators

#	Name	*d* (μm)	*s* (μm)
1	TF_250_200	250	200
2	TF_250_100	250	100
3	TF_250_40	250	40
4	TF_200_100	200	100
5	TF_100_100	100	100

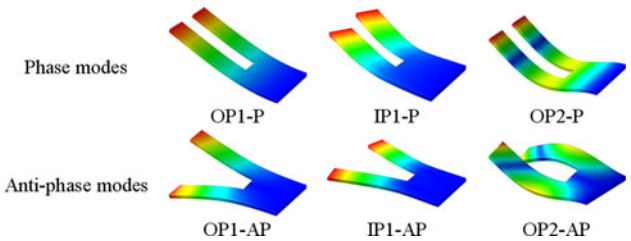

Fig. 2 Graphical representation of the modal shapes for the considered modes. *OP* refers to out-of plane modes and *IP* to in-plane modes. Phase and anti-phase modes are labeled as *P* and *AP*, respectively. *Tones* indicate the displacement magnitude

Table 2 Z-direction displacement for each mode with different signal distributions

Excitation				Z-displacement (pm) TF_250_200					
1	2	3	4	OP1-P ++++	OP1-AP ++−−	IP1-P	IP1-AP	OP2-P ++++	OP2-AP ++−−
+	+	−	−	5.73	**482.40**	3.92	1.58	0.77	**32.18**
+	−	+	−	6.46	8.69	**5.02**	*0.69*	–	*2.07*
+	−	−	+	*1.39*	*5.24*	*0.41*	**9.30**	–	2.04
+	+	+	+	**429.59**	63.34	1.14	2.03	**4.78**	4.52

Bold and italic values correspond to maximum and minimal values of the displacement, respectively, for each mode. The applied signal is indicated for electrodes (1, 2, 3 and 4). The reference signal is labeled as (+) and the 180°-shifted one as (−). The optimal configuration for each case is indicated under the mode name

Table 3 X-direction displacement for each mode with different signal distributions

Excitation				X-displacement (pm) TF_250_200					
1	2	3	4	OP1-P	OP1-AP	IP1-P +−+−	IP1-AP +−−+	OP2-P	OP2-AP
+	+	−	−	–	**34.78**	48.39	25.66	–	**3.54**
+	−	+	−	–	1.03	**63.18**	*10.20*	**0.82**	*0.51*
+	−	−	+	1.41	–	*2.75*	**158.58**	–	0.68
+	+	+	+	**23.75**	4.32	11.29	31.74	0.63	0.70

Bold and italic values correspond to maximum and minimal values of the displacement, respectively, for each mode. The optimal configuration for each case is indicated under the mode name

mentioned, the top metallization has four longitudinal independent electrodes (see Fig. 1). Each arm can be divided into two longitudinal halves, covered by an electrode. In out-of-plane modes, the bending of the two parts of each arm occurs in the same direction, so the stress sign on both halves is the same on each y-plane and, hence, the best configuration is (++++) or (++−−) for the two prongs in phase or anti-phase, respectively. On the contrary, in the case of in-plane modes, each half of the cantilever suffers stress of different sign. One of the halves suffers compression in the y-direction, whereas the other part is expanding. In-plane modes, thus, require opposite sign of the excitation signal on the two electrodes of each arm, i.e. (+−+−) or (+−−+) for phase or anti-phase modes, respectively.

The characterization of the resonators has been performed with a Doppler vibrometer, which determines the displacement of the resonator for each mode. The kind of signal we employ is a periodic chirp with 2V of maximal amplitude, which allows a quick characterization in frequency. The displacement has been measured in the x and z directions (see Fig. 1). Tables 2 and 3 summarize the displacements obtained with the different signal distribution for each of the studied modes, which corroborate the deductions about the optimal excitations done taking into account the modal shapes. The results shown here correspond to a tuning fork of type number 1 (TF_250_200). IP modes have been included in the table with z-displacement and OP modes in the one with x-displacements, in order to account for the contribution of the orthogonal direction in each case.

As can be seen in Table 2, the best configuration to excite OP phase modes is, as expected, the application of the same signal to all four electrodes (++++). On the other hand, the displacement for OP anti-phase modes is maximized when the signals applied to each of the arms are shifted 180° (++−−). In-plane modes require different signals applied on each of the electrodes lying on the same arm (see Table 3). The alternation of shifted and not shifted signals on the four electrodes maximizes the displacement of the IP-phase mode (+−+−). The IP-anti-phase mode, however, is excited when the reference signal is applied to the external electrodes and the shifted one is applied to the internal ones (+−−+). It can be seen in Tables 2 and 3 that out-of-plane modes show some displacement along x and in-plane modes some displacement in z.

The measurements in the x direction confirm the expected results: for the in-plane modes, the displacements in the x direction are much larger than in the z direction. On the other hand, the displacements in the x direction for the out-of-plane modes are not significant in comparison with those obtained for the z direction. In Figs. 3 and 4, we represent for each mode the displacements obtained with the different signal configurations, illustrating the previous affirmations.

In Figs. 3, 4 and 5 the displacements in the z direction for the out-of-plane (OP) modes, and the x direction for the in-plane (IP) modes are shown as a function of frequency for the different signal distributions. The displacements in the x and z directions are also compared for the optimal excitation in Fig. 4.

Graphs in Fig. 3 illustrate graphically the optimization of the excitation of each mode achieved when the right signal configuration is employed. In most of the cases the displacement measured with the optimal excitation is much higher than in all other cases and there are configurations which inhibit some modes almost totally. This is the case of mode OP1-AP, for example, which is shown in Fig. 3b. The optimal configuration is, as expected, the one applying 180°-shifted signals to each of the arms (++−−). The displacement obtained in this case is increased in a factor higher than four, with respect to the one obtained with the homogeneous excitation (++++) and above forty times bigger than with the other two configurations. These results corroborate the selective modal excitation intended with the design of the split electrode.

The comparison of the x and z-displacements confirms the fact that the displacement in the z direction for the in-plane modes is almost zero. This makes it difficult to detect the in-plane modes when only measurements of the displacement in the z direction can be done. For the out-of-

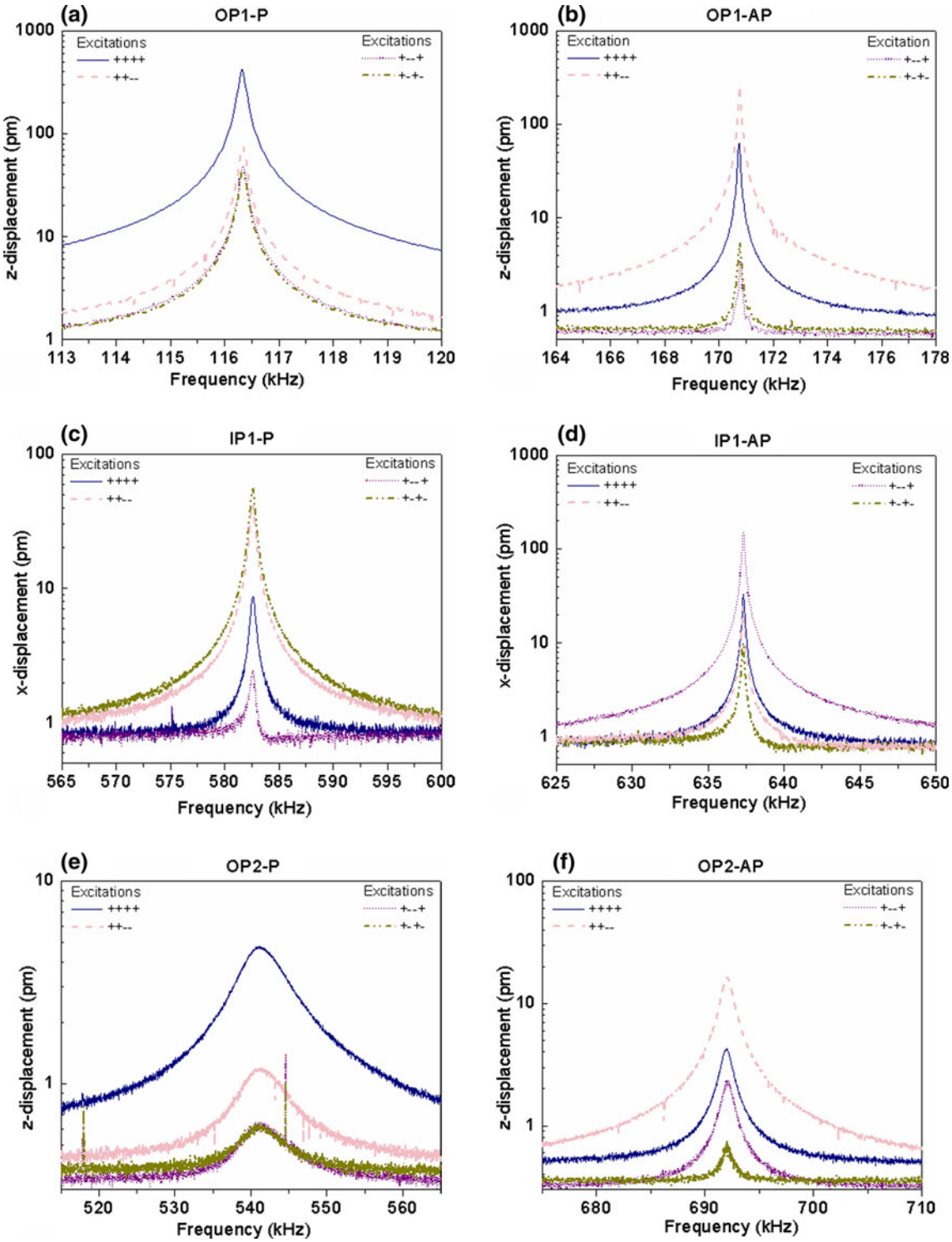

Fig. 3 Doppler vibrometer measurement of the displacement in the z-direction for the considered vibration modes of the tuning fork TF_250_200 employing four different signal configurations. **a** OP1-P mode. **b** OP1-AP mode. **c** IP1-P mode. **d** IP1-AP mode. **e** OP2-P mode. **f** OP2-AP mode

plane modes, the x-displacement is negligible when compared to the z-displacement.

Finite Element simulations using commercial software have been performed to investigate the ratio between the x- and z-displacements for an OP and an IP mode. The simulation results are shown in Fig. 5 and compared with the measurements in Table 4. We defined the magnitude u to account for the maximal z-displacement and v for the

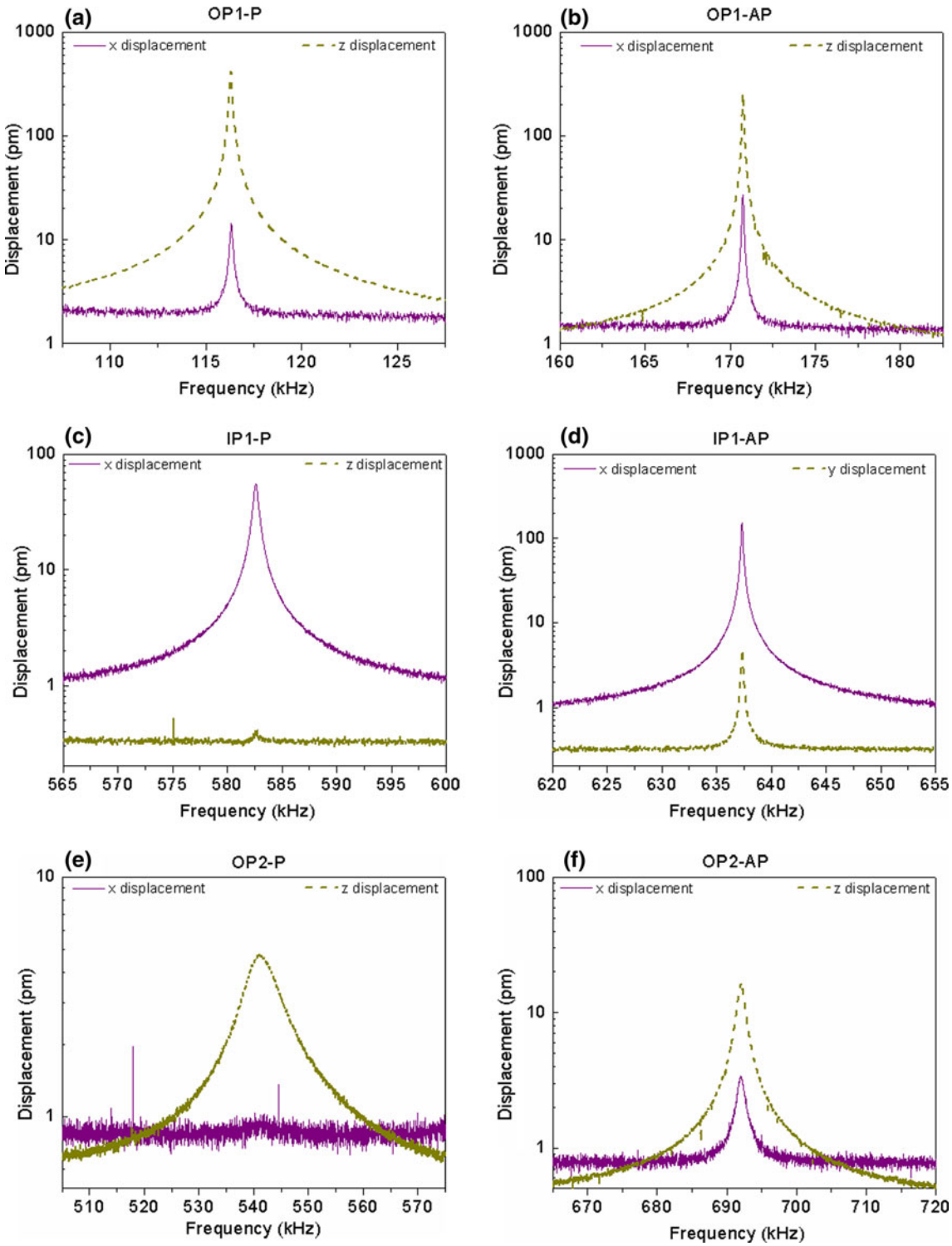

Fig. 4 Comparison between the measured z and x-displacement for the considered vibration modes of the tuning fork TF_250_200 with different actuation signal distributions. **a** OP1-P mode. Actuation: ++++. **b** OP1-AP mode. Actuation: ++−−. **c** IP1-P mode. Actuation: +−+−. **d** IP1-AP mode. Actuation: +−−+. **e** OP2-P mode. Actuation: ++++. **f** OP2-AP mode. Actuation: ++−−

maximal x-displacement. We obtained the ratio of the displacement in the main vibration direction divided by the displacement in the orthogonal direction. This is $T = u/v$ for OP modes and $T^{-1} = v/u$ in the case of IP modes. It can be seen in Table 4 that for both modes the ratios T and T^{-1} are significantly higher in the measurements. This can be attributed to discrepancies between nominal and real dimensions, as well as misalignments occurred during

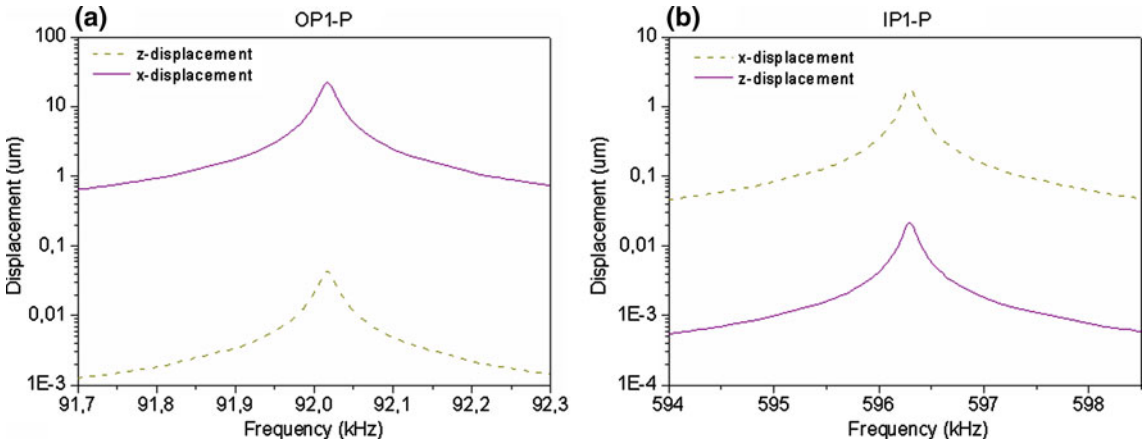

Fig. 5 Comparison between the simulated z and x-displacement for two phase modes of the tuning fork TF_250_200. **a** OP1-P mode with signal distribution ++++. **b** IP1-P mode with actuation signal distribution +−+−

Table 4 Comparison between the measurement and simulation results of the ratios (T and T^{-1} of the z- and x-maximal displacements (u and v, respectively) for the OP1-P and IP1-P modes

TF_250_200	Simulation	Measurement
OP1-P mode: $T = u/v$	1.96×10^{-3}	55.3×10^{-3}
IP1-P mode: $T^{-1} = v/u$	1.21×10^{-2}	7.95×10^{-2}

fabrication. These irregularities cause asymmetries in the devices and spurious displacements in other than in the main vibration direction and are not taken into account in the simulated ideal model. Nevertheless, the spurious displacements are not null in any of the cases, as is corroborated by the simulations.

Regarding the resonance frequencies, except in certain cases, the experimental and simulation results show an acceptable agreement (see Table 5). The mismatch between expected and measured values appreciated in some of the frequencies, can be attributed to fabrication tolerances, given that the actual dimensions do not agree perfectly to the nominal values used in the simulations and that slight misalignments occur frequently during fabrication.

Taking into account these results, we can try to infer certain tendencies in the influence of s and d on the resonance frequencies. We will take into account the frequencies predicted in the simulations, f_s. Let us first focus on the first three resonators, in which the length of the anchor area, d, has been maintained constant, whereas the distance between the arms, s, takes the values 200, 100 and 40 μm. The differences in the frequencies are not very important, but we can observe that, for the phase modes, the frequencies decrease as s decreases. However, the effect is just the opposite for the anti-phase modes. If we now consider the last three resonators (TF_250_100 is repeated for a better comparison of the frequencies) in which d has been

Table 5 Measured (f_m) and simulated (f_s) resonance frequencies of each mode for resonators with different dimensions

TF_d_s	OP1-P frequencies (kHz)		OP1-AP frequencies (kHz)		OP2-P frequencies (kHz)	
	f_m	f_s	f_m	f_s	f_m	f_s
TF_250_200	116	91	170	112	541	455
TF_250_100	59	83	102	123	306	452
TF_250_40	92	77	198	134	519	448
TF_250_100	59	83	102	123	306	452
TF_200_100	65	96	98	125	341	537
TF_100_100	78	130	93	136	453	781
TF_d_s	IP1-P frequencies (kHz)		OP2-AP frequencies (kHz)		IP1-AP frequencies (kHz)	
	f_m	f_s	f_m	f_s	f_m	f_s
TF_250_200	582	594	692	523	637	615
TF_250_100	540	575	414	557	624	618
TF_250_40	492	543	755	592	644	620
TF_250_100	540	575	414	557	624	618
TF_200_100	564	596	443	624	622	620
TF_100_100	593	641	512	803	609	646

TF_250_100 is repeated in the second and fourth positions for a better comparison

modified, we can observe the same tendency for all modes: the smaller d is, the higher the resonance frequency of the mode gets. In this second case, the influence on the resonance frequency is higher, so it is more convenient to modify d to change the resonance frequency. If we take into account the values obtained experimentally, the mentioned tendencies cannot be observed, likely due to the fact that the errors introduced by the deviations from the nominal

Table 6 Comparison of the frequency shift between the anti-phase (f_{AP}) and phase (f_P) resonance frequencies for the modes OP1, IP1 and OP2

TF_*d*_*s*	$\Delta f = f_{AP} - f_P$					
	OP1		OP2		IP1	
	Δf_m	Δf_s	Δf_m	Δf_s	Δf_m	Δf_s
TF_250_200	54	21	151	68	55	21
TF_250_100	43	40	108	105	84	43
TF_250_40	106	57	236	144	52	77
TF_250_100	43	40	108	105	84	43
TF_200_100	33	29	102	87	58	24
TF_100_100	15	6	59	22	16	5

For each mode, the measurement (Δf_m) and simulation (Δf_s) results are indicated. TF_250_100 is repeated in the second and fourth positions for a better comparison

dimensions due to the fabrication process have a larger influence on the resonance frequencies. Nevertheless, if we take into account the difference between the frequencies of the anti-phase and phase resonances ($\Delta f = f_{AP} - f_P$), for each of the modes (see Table 6), we can observe that the Δf varies when the dimensions d and s are modified and this can be observed in the simulation and, except in certain cases, also in the measurement results. It is expected that, in samples with a larger coupling between both arms of the tuning fork, the separation between the phase and anti-phase modes is bigger than in those in which the coupling is not so important (Castellanos-Gómez et al. 2009). This occurs, for example, in the resonators with a small separation between the arms, s. For the resonator with $s = 40$ μm, the frequency shift is considerably larger than for the resonator with $s = 200$ μm. On the other hand, in those tuning forks in which the length of the anchor area, d, is increased, the phase and anti-phase resonances split apart, given that the increase of d enhances the coupling.

4 Quality factors

As previously mentioned, the quality factor (Q) of a resonator is a key parameter regarding its application as sensing devices. It is especially important in those applications involving viscous media, since damping is highly increased and only resonators with high quality factors are capable of working under such conditions. This is the reason why this resonator was specially designed to optimize the in-plane modes, since such modes suffer a lower damping in liquid media (Beardslee et al. 2010). Once the optimization of in-plane modes has been confirmed by the experimental results, it is necessary to determine the quality factor of the resonator. We have estimated the quality factor in air of each of the modes for the different samples from the measurements of the displacement (see Table 7). The results prove that, in all cases, anti-phase modes have a higher quality factor than their phase counterparts. This could be attributed to the fact that in anti-phase modes, forces at the attachment area have opposite directions and propagating waves are cancelled, considerably reducing support losses (Vignola and Judge 2008). A deeper study on the influence of this and other factors determining the quality factor of the resonator should be performed in order to determine the relative influence of anchor, viscous, acoustic or other loss mechanisms. Nevertheless, simulations taking into account only anchor losses have been carried out, confirming this tendency for the phase and anti-phase modes. This difference in the quality factors of the phase and anti-phase modes is quite significant and it even achieves a factor close to 9 in some cases. The variation of the dimensions d and s has no clear influence in the experimental values of the quality factors.

Table 7 Estimated Q-factor values of the considered vibration modes for each studied resonator in air

Quality factor						
TF_*d*_*s*	OP1-P	OP1-AP	IP1-P	IP1-AP	OP2-P	OP2-AP
TF_250_200	865	2,112	1,428	4,344	72	642
TF_250_100	685	1,060	1,543	3,524	442	1,276
TF_250_40	1,060	2,169	820	4,143	186	1,430
TF_200_100	622	1,012	965	3,550	817	1,290
TF_100_100	677	927	1,222	2,901	419	1,152

For all the studied resonators, the highest quality factor is achieved for the in-plane anti-phase mode, with values above 4,000. These values are at least twice as high as values obtained for an out-of-plane mode of the same tuning fork. The highest Q values measured in a cantilever with similar dimensions and fabricated following the same process are around 1,400 for the torsional mode "mode (11)" following Leissa's nomenclature (Leissa 1969) and 3,100 for the first in-plane mode. Values around 3,000 have been reported for similar cantilevers optimized for in-plane vibration (Leighton et al. 2007). The high achieved Q values make these resonators good candidates for their application in liquid media. Work is in progress in this direction in order to confirm the suitability of these resonators for that purpose.

5 Conclusions

A complete study of the six first vibration modes of a piezoelectric tuning-fork has been carried out. Selective excitation of the modes is done applying different signal

configurations, which combine 180°-shifted signals on four independent electrodes. The exhaustive characterization performed using a Doppler vibrometer confirms the maximization of the displacement when the optimal excitation for each mode is employed. The influence of the resonator geometry on the performance of the tuning-forks has been studied on five devices with different dimensions. The coupling is higher in the resonators in which the microcantilevers are closer or the anchor area is longer, causing a larger frequency split between the frequencies of the phase and anti-phase modes. The quality factor of the studied modes has been estimated. It has been observed that all anti-phase modes present higher Q values than their phase counterparts. Additionally, in-plane modes have larger quality factors, so the highest value corresponds to the in-plane anti-phase mode, which is above 4,300. Additional work is in progress in order to reduce the effect of different loss contributions and further increase the quality factor of the resonators. The characterization and application in liquid environments is envisaged.

Acknowledgments This work has been supported by Junta de Comunidades de Castilla-La Mancha project no PEIC11-0022-7430. MICINN (Spain) supported by project contract DPI2009-07497, a FPI Grant (Ref. BES-2010-030770) awarded to Tomás Manzaneque and a Juan de la Cierva research contract awarded to Marta Gil (JCI-2009-04502). The authors would also like to thank Dr. Erwin Peiner (Technical University of Braunschweig) for the support during device fabrication.

References

Beardslee LA et al (2010) Geometrical optimization of resonant cantilevers vibrating in in-plane flexural modes. IEEE Sens 2010:1996–1999

Castellanos-Gómez A, Agraït N, Rubio-Bollinger G (2009) Dynamics of quartz tuning fork force sensors used in scanning probe microscopy. Nanotechnology 20:215502

Dufour M, Heinrich SM, Josse F (2007) Theoretical analysis of strong-axis bending mode vibrations for resonant microcantilever (bio) chemical sensors in gas or liquid phase. J Microelectromech Syst 16:1

Karrai K, Grober RD (2005) Piezoelectric tip-sample distance control for near field optical microscopes. Appl Phys Lett 66(14):1842–1844

Leighton GJT, Kirby PB, Fox CHJ (2007) In-plane excitation of thin silicon cantilevers using piezoelectric thin films. Appl Phys Lett 91:183510

Leissa AW 1969 Vibration of plates NASA Technical Report SP160

Momosaki E (1997) A brief review of progress in quartz tuning fork resonators. In: Proceedings of the 1997 IEEE international frequency control symposium, pp 552–565

Sánchez-Rojas JL et al (2010) Modal optimization and filtering in piezoelectric microplate resonators. J Micromech Microeng 20:055027

Vignola JF, Judge JA (2008) Architectural considerations of micro- and nanoresonators for mass detection in the presence of a fluid. J Appl Phys 104:124305